

06110-6-I

THE UNIVERSITY OF MICHIGAN
COLLEGE OF ENGINEERING
DEPARTMENT OF NUCLEAR ENGINEERING
LABORATORY FOR FLUID FLOW AND HEAT TRANSFER PHENOMENA

Internal Report No. 6

GAS BUBBLE ENTRAINMENT IN WATER AND MERCURY
VERSUS GAS CONTENT

M. J. Robinson
F. G. Hammitt

January, 1965

ACKNOWLEDGEMENTS

The financial support for this investigation was furnished by the Atomics International Division of North American Aviation, Inc., under Contract No. N41S6BA-002006. The authors would also like to acknowledge the assistance of D. Ericson who furnished some of the data herein.

ABSTRACT

An experiment is described in this report involving photographs of flow of water and mercury with entrained gas to obtain data on visible bubble sizes and visible gas content for known loop operating parameters and known total gas content. From a comparison of the estimated visible gas content and the known total gas content conclusions are drawn regarding the distribution between dissolved and entrained gas. Conclusions are also presented regarding smallest visible bubble sizes, average mean observed sizes in both fluids, and homogeneity of the gas distribution in the fluids.

TABLE OF CONTENTS

ACKNOWLEDGEMENTS.....	ii
ABSTRACT.....	iii
LIST OF TABLES.....	v
LIST OF FIGURES.....	vi
I. INTRODUCTION.....	1
II. EXPERIMENTAL PROCEDURE.....	2
III. DATA REDUCTION AND ANALYSIS.....	4
A. WATER LOOP.....	4
B. MERCURY LOOP.....	9
IV. BUBBLE RADIUS CONSIDERATIONS.....	12
V. CONCLUSIONS.....	16
APPENDIX.....	17
BIBLIOGRAPHY.....	26

LIST OF TABLES

<u>Table</u>	<u>Page</u>
I Water and Mercury Loop Operating Parameters for This Investigation.....	5
II Air Content and Photograph Number Versus Time for Water Loop.....	6
III Bubble Radius and Gas Content Data in "Dry" Mercury	14

LIST OF FIGURES

<u>Figure</u>		<u>Page</u>
1	Air Content and Photograph Number versus Time.....	20
2	Photograph Number 1 of Water Loop at 3.42% by Volume Air, Magnification 1X. (11/18/64).....	21
3	Photograph Number 2 of Water Loop at 3.42% by Volume Air, Magnification 2X, (11/18/64).....	21
4	Photograph Number 3 of Water Loop at 2.85% by Volume Air, Magnification 2X, (11/20/64).....	22
5	Photograph Number 4 of Water Loop at 2.92% by Volume Air, Magnification 2X, (11/20/64).....	22
6	Photograph Number 5 of Water Loop at 2.95% by Volume Air, Magnification 2X, (11/20/64).....	22
7	Photograph Number 6 of Water Loop at 2.95% by Volume Air, Magnification 2X, (11/20/64).....	23
8	Photograph Number 7 of Water Loop at 2.85% by Volume Air, Magnification 2X, (11/20/64).....	23
9	Photograph Number 8 of Water Loop at 2.45% by Volume Air, Magnification 2X, (11/20/64).....	23
10	Photograph Number 9 of Water Loop at 2.45% by Volume Air, Magnification 2X, (11/20/64).....	24
11	Photograph Number 10 of Water Loop at 2.07% by Volume Air, Magnification 2X, (11/20/64).....	24

LIST OF FIGURES (continued)

<u>Figure</u>		<u>Page</u>
12	Photograph Number 11 of Water Loop at 2.07% by Volume Air, Magnification 2X, (11/20/64).....	24
13	Standard Cavitation in Mercury at 33 ft/sec at a Gas (Argon) Content of 1.8 ppm. Average Bubble Radius in Throat is 7.9 mils. Magnification 1X.	25

I. INTRODUCTION

The condition of the gas within both the mercury and water facilities, i.e., the portion of gas which is entrained as opposed to dissolved or simply trapped in a static condition, as in a stagnant pocket along the top of a horizontal pipe; its distribution in the stream; the mean bubble size and bubble size spectrum; etc., are questions which closely relate to the applicability and generality of the cavitation number vs. gas content data acquired in the present investigation. These detailed questions relating to the gas disposition are also important from the viewpoint of cavitation damage.

The experiment described in the present report involves photographs of the flow in both the water and mercury facilities taken to obtain some data on visible bubble sizes and their number density for known loop operating parameters and total loop gas content. From a comparison of the estimated total gas in visible bubbles to the known total gas content it is possible to draw some conclusions regarding the distribution between dissolved and entrained gas.

II. EXPERIMENTAL PROCEDURE

The experimental procedure followed to obtain the present water data was as follows. The water loop was filled with fresh tap water, started, and allowed to run for about 1 hour. No bubbles were then visible in the venturi throat so air was artificially injected into the stream in a somewhat continuous manner by loosening one of the venturi specimen holders. Since the venturi wall pressure at the location of the specimen holders for the selected operating conditions was less than atmospheric, air was drawn into the venturi at that point. This procedure was continued until the visible presence of air bubbles in the venturi persisted after re-sealing of the specimen holder opening, i.e., the opening was closed and the throat section of the venturi observed for twenty to thirty minutes. When it was observed that bubbles continued to remain visible, the experiment was started.

First a photograph, (1.2 microsecond exposure time), was taken of the flow in the throat section and then a sample of the water was obtained and analyzed in the Van Slyke apparatus for total air

content (dissolved + entrained). It should be noted that when there are visible bubbles in the sampling bottle, some of them have a chance to escape before the sample is transferred to the Van Slyke. With this in mind the Van Slyke data must be, in this case, less than or equal to the actual gas content. At this point the deaerator was activated and the time recorded so that the air content versus time could be plotted. Subsequently, repeated photographs of the venturi throat section and air content determinations were made, and the times recorded, until there was no longer any visible appearance of bubbles. From the resulting data it was possible to establish a value of air content corresponding to the disappearance of all visible voids in the venturi throat for this particular experiment. Since the prior history of the water appears to have considerable influence on the distribution between dissolved and entrained air, such results may depend closely on the precise experimental procedure followed. Also the size of the smallest visible voids in the venturi throat could be determined.

III. DATA REDUCTION AND ANALYSIS

A. Water Loop

Table I shows the loop performance and operating conditions under which this experiment was conducted. The water velocity in the throat was approximately 100 feet per second and the cavitation condition was "standard", so that any air in the loop should have been well mixed upon traversing the cavitating region. This does not, however, guarantee that the air content throughout the whole system was homogenous.

Table II lists the air content and photograph numbers with their respective times. Figure 1 presents the same data in curve form. The slight increase of air content versus time for the first two readings after startup was likely due to non-homogeneity of the overall air content in the loop. Another possible explanation is that the bubbles in the first two samples were larger and more were lost while transferring the sample from the loop to the Van Slyke. However, the air content did decrease from about 3% by volume to about 2 % by volume during the experiment.

Table I

Water and Mercury Loop Operating Parameters for This Investigation

<u>Parameter</u>	<u>Water</u>	<u>Mercury</u>
RPM	1650	1500
Pump Discharge Pressure	59.0 psig	139.0 psig
Pump Suction Pressure	31.0 psig	-5.7 psig
Throat Velocity	97.2 fps	33.0 fps
Venturi Inlet Pressure	58.5 psig	97.0 psig
Venturi Outlet Pressure	36.0 psig	69.0 psig
Fluid Temperature	60°F	91°F
Cavitation Condition	Standard	Standard
Reynolds' No. (based on throat diameter)	3.05x10 ⁵	11.8x10 ⁵

Table II

Air Content and Photograph Number Versus Time for
Water Loop

<u>Time</u>	<u>Van Slyke Reading</u>	<u>Temp. (°C)</u>	<u>Air Content % by Volume</u>	<u>Photograph Number</u>	<u>Date</u>
3:00 P.M.	272 mm Hg	18	3.42	1 & 2	11/18/64
2:23 "				3	11/20/64
2:25 "	246	17	2.85	-	"
2:30 "	Deareator turned on at this time.				"
2:40 "	249	17	2.92	4	"
2:45 "				5 & 6	"
2:49 "	253	17	3.03	-	"
2:50 "				7	"
2:55 "	238	17	2.63		"
2:59 "				8 & 9	"
3:09 "	219	17	2.12	-	"
3:11 "				10 & 11	"

A single point is shown on Figure 1 at the top left at an air content of about 3.4%, and two photographs, numbers 1 and 2, were taken at that condition. This data was taken on 11/18/64, two days prior to the more complete investigation, in order to develop the photographic technique. The air content is larger in this instance, as the loop was started with large air voids showing in the venturis. This air was circulated and mixed in the loop to be sure there would be some visible air voids in the venturi to use for the photographic checkout. Figures 4 through 12, (photograph numbers 3 through 11), were taken on 11/20/64 in connection with the experiment as described earlier. Upon examination of these photographs it seems that for air contents of the order of 3.0% by volume and higher, enough entrained air is present to form a continuous, (but very dilute), cloud of visible bubbles. Then as the air content decreases, Figures 7 through 10, the appearance of air is confined to isolated patches and bubbles. Finally as the air content approaches saturation at STP (about 2.0%) the disappearance of air bubbles in the throat is noted, and also the cavitation cloud just visible at the far right in the photographs becomes more transparent

and "thinner" in appearance. Since the pressures throughout the water facility vary substantially around the loop, there is no significant specific region where standard pressure (1 atm.) prevails. Hence the condition of saturation based on STP may not be of special significance.

An attempt was made to determine the volume of air visible in Figure 3 by visual inspection of the photograph. A region on the photograph, 1 inch in diameter by 2½ inches long and located in the throat area, was examined; 170 bubbles were counted with an estimated mean diameter of 32 mils. Thus, since the photograph magnification is 2X, the volume of water in the examined area is;

$$V_{H_2O} = \frac{\pi (\frac{1}{2})^2}{4} \text{ in}^2 \times \frac{5}{4} \text{ in} = 0.245 \text{ in}^3$$

and the actual bubble radius is then 8 mils, so the bubble volume is;

$$V_{\text{air}} = \frac{4}{3} \pi (.008)^3 \times 170 = 3.65 \times 10^{-4} \text{ in}^3$$

and the % by volume of entrained air in visible form is then;

$$\% \text{ by volume} = \frac{3.65 \times 10^{-4}}{2.45 \times 10^{-1}} \times 10^2 = 0.148\%$$

Since the Van Slyke reading for total air content was 3.42% by volume for this same case, the difference is then 3.42 - 0.148 or 3.27% which must then be either in solution or in an entrained form such as smaller bubbles not visible to an observer. It has also been estimated from the photographs that bubbles down to about 3 mils diameter can be detected.

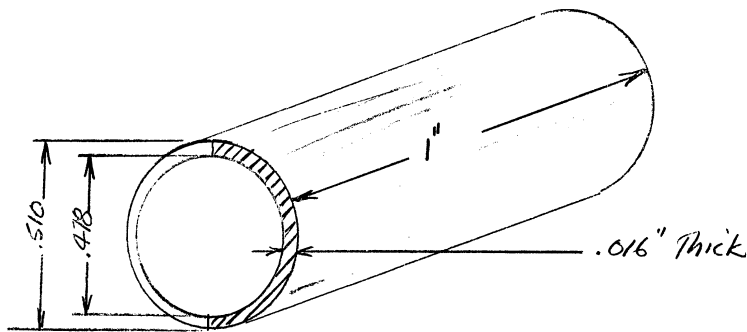
B. Mercury Loop

Figure 13 is a photograph, about 1:1 scale, of the venturi throat section in the mercury loop during a particular gas injection run reproduced from reference (1), and was re-analyzed to obtain data similar to the above water data. A Van Slyke determination of the gas mass showed 1.8 ppm of argon. In the photograph for a 1 inch long section of the throat approximately 200 bubbles with a mean radius of 7.9 mils* were counted. Thus the volume of visible gas under consideration is;

$$V_{\text{gas}} = \frac{4}{3} \pi (7.9)^3 \times (10^{-3})^3 \times 200 = 4.12 \times 10^{-4} \text{ in}^3$$

* It is interesting to note that the estimated mean bubble radii in the venturi throat (i.e., low pressure region) is approximately the same for water and mercury.

Since the mercury is opaque (as opposed to water) the above amount of gas was assumed to be in a mercury volume approximately one bubble diameter thick adjacent to one side of the venturi wall (see sketch below). The following model has then been assumed for the total mercury volume in which the gas was observed:



$$V_{\text{Hg}} = \pi \frac{(.510^2 - .478^2)}{4} \text{ in}^2 \times \frac{1}{2} (\text{one side visible in photo}) \times 1 \text{ in}$$

$$V_{\text{Hg}} = 1.26 \times 10^{-2} \text{ in}^3$$

and then the % by volume is:

$$\% \text{ by volume} = \frac{4.12 \times 10^{-4}}{1.26 \times 10^{-2}} \times 10^2 = 3.27\%$$

To convert to ppm by mass, the density of the gas (argon) is required at the applicable pressure.

At STP:

$$\rho_{\text{air}_{\text{STP}}} = 1.29 \times 10^{-3} \text{ gm/cc}$$

$$\rho_{\text{argon}_{\text{STP}}} = (40/29) \times \rho_{\text{air}} = 1.74 \times 10^{-3} \text{ gm/cc}$$

The average observed pressure in the throat at the location examined was $(-11.05 + -10.1)/2^{(2)}$ psig or -10.6 psig or 4.1 psia. Since the mean bubble diameter was 16 mils, the pressure inside the bubbles is greater than the adjacent fluid pressure by the surface tension effect,

$$\Delta P = 4\sigma/D \text{ or, } \Delta P = (4 \times .0318 \text{ lb/ft}) / (.016/12) \text{ ft} = 95.5 \text{ lb/ft}^2 = 0.66 \text{ psi}$$

Thus the argon is under a pressure of about $(4.1 + 0.66) = 4.76$ psia and its density then is;

$$\rho_{\text{argon}} = 1.74 \times 10^{-3} \text{ gm/cc} \times (4.76/14.7) = .565 \times 10^{-3} \text{ gm/cc}$$

and the ppm by mass is:

$$\text{ppm} = (0.0327 \times .565 \times 10^{-3}) \times 10^6 / 13.6 = 1.36 \text{ ppm}$$

Considering the relatively gross nature of the assumptions, this estimate agrees relatively well with the measured value of 1.8 ppm.

The above calculation then is consistent with the assumption that the gas in the mercury loop is approximately uniformly and well dispersed, and is essentially all in the entrained form.

IV. BUBBLE RADIUS CONSIDERATIONS

Some additional data has been obtained and analyzed on calculated bubble radius values versus gas content in the mercury facility since the issuance of the last report.⁽¹⁾ The data was obtained in the mercury facility with the $\frac{1}{2}$ " venturi, at a throat velocity of 33.1 feet per second and for a gas content range of 0.811 ppm to 1.382 ppm air. The corresponding calculated bubble radius values, from nine observations, ranged from 0.24 mils up to 0.39 mils (Table III). This data cannot be related directly to the observed visible bubble sizes reported herein as the gas content as measured for these bubbles was larger, i.e., 1.8 ppm, so that presumably the bubble size would be somewhat greater.

While most of the gas has been shown to exist in mercury as visible bubbles, (previous section of this report) a small percentage was unaccounted in this fashion. If one assumes that this small discrepancy is in the form of bubbles below the visible size range, the number of such smaller bubbles could be quite large. A very hypothetical estimate is presented in the Appendix, based on this

particular set of data, in which a possible order of magnitude for the number of such micro-bubbles was obtained, consistent with the small percentage of gas not found in visible bubbles. Assuming a mean bubble radius of 0.1 mils for the non-visible bubbles, a very small amount of gas (the unaccounted for 0.44 ppm) requires 2.25×10^8 such bubbles per cubic inch of mercury. If a 1 mil mean radius is assumed (i.e., on the threshold of visibility) then 1.23 million bubbles per cubic inch are required. It is thus quite evident that, while the amount of gas entrained in a liquid metal as mercury in the form of micro-bubbles may be quite small, there still may exist an enormous number of possible cavitation nucleation sites,* even if there is no visible indication of gas in the liquid. While the present data indicates the presence of very large numbers of micro-bubbles, a further calculation shows that these are still relatively remote from each other. For example, within a one inch cube there could be a maximum of $\sim 10^{12}$ bubbles of 0.1 mil diameter versus the present estimate of $\sim 10^8$, so the mean

* It is generally assumed that active cavitation nucleation sites in a flowing liquid must be the order of 0.1 to 1 mil in radius. The underpressure required to activate much smaller sites is too great to be consistent with the measured pressures.

Table III

Bubble Radius and Gas Content Data in "Dry" Mercury

<u>Run No.</u>	<u>Gas</u>	<u>Average ppm</u>	<u>Bubble Radius - inches</u>
17	Air	0.904	0.0002409
18	Air	0.811	0.0002840
19	Air	1.382	0.0003918
20	Air	1.058	0.0003514
21	Air	1.308	0.0003759
22	Air	0.851	0.0002881
23	Air	0.879	0.0003144
24	Air	0.860	0.0003851
25	Air	1.120	0.0003544

bubble spacing would still be ~ 25 diameters. Similarly for the 1 mil bubbles there could be a maximum of 10^9 , and the present estimate is $\sim 10^6$ so that the mean spacing would be about 10 diameters. Since there are $\sim 10^9$ molecules of argon in a 0.1 mil bubble, the gas is still a continuum so that the fluid relations can be applied.

Considering again the mean visible bubble diameter of 8 mils (Figure 13) and calculating the diameter for such a bubble at the pressure of the gas content capsule (where the calculated bubble diameters apply, essentially the venturi outlet pressure) we obtain, assuming an isothermal process:

$$(P_{ST_1} + 2\sigma/r_1)r_1^3 = (P_{ST_2} + 2\sigma/r_2)r_2^3$$

where,

P_{ST_1} and P_{ST_2} are the static pressures in the liquid around the bubbles

r_1 = radius of bubble in gas content capsule (high pressure region)

r_2 = radius of bubble in venturi throat (low pressure region)

σ = surface tension of mercury

Using the measured or assumed values, $r_2 = 8$ mils, $P_{ST_2} = 4.1$ psia, $P_{ST_1} = 80$ psi and $\sigma = .0318$ lb/ft, 3 mils was determined for the bubble radius in the

capsule. This is much larger than the values calculated via the computer program from the actual Van Slyke data (Table III). It is felt that this further substantiates the existence of very many bubbles of a size smaller than the minimum visible range of 1 to 3 mils, i.e., the effective mean bubble radius is substantially smaller than the arithmetic mean which has been used in these calculations since the numerical distribution must be biased toward the smaller size. It is hoped to obtain a more precise bubble size spectrum from further detailed examination of the photographs at a later date.

V. CONCLUSIONS

i) The appearance of visible bubbles in the water loop venturis seems to be limited to air contents for the water at standard temperature and pressures which are equal to or greater than STP saturation.

ii) The mean visible bubble radii observed in water at ~ 100 ft/sec and in mercury at ~ 33 ft/sec for large gas contents are about the same (8 mils). Reynolds' numbers for the two specific cases analyzed are the same order of magnitude, i.e., $Re_{Hg} = 11.8 \times 10^5$ and $Re_{H_2O} = 3.05 \times 10^5$.

iii) Only about 5% of the measured gas content in the water can be accounted for as visible entrained bubbles, vs. nearly all in the mercury case. However, it is likely that many bubbles exist in water and mercury at diameters less than 1 to 3 mils. In fact the mean bubble size in mercury estimated from considerations of surface tension is ≈ 1 mil.

iv) The gas injected into either fluid is well and reasonably dispersed uniformly throughout the fluid.

v) Most of the gas in the water is in solution, while essentially all of the gas in the mercury is entrained.

vi) Preliminary estimations on non-visible bubble numbers indicate that there may well be literally millions of micro-bubbles per in^3 of fluid. However, these would contain only a small percentage of the known gas content.

APPENDIX

An attempt is made below to determine a possible realistic value for the number of bubbles below the visible size range in the mercury flow of Figure 13. Taking the difference in the observed visible mass percent, (1.36 ppm), and the total mass content,

as determined from the more accurate Van Slyke apparatus, (1.80 ppm), it is probable that an amount of argon exists, in the form of entrained micro-bubbles of a size less than the visible range of:

$$1.80 - 1.36 = 0.44 \text{ ppm}$$

or,

$$0.44 \text{ ppm} \times 10^6 \times 1.26 \times 10^{-2} \text{ in}^3 \times 13.6 \text{ gms/cc} \\ \times 16.4 \text{ cc/in}^3 = 1.24 \times 10^{-6} \text{ gms.}$$

Thus, the total mass of argon unaccounted for is 1.24×10^{-6} gms.

Now assume a mean small bubble radius of 0.1 mil.

The volume of such a bubble would be;

$$V_{\text{bubble}} = (4/3) \pi (0.1)^3 \times 10^{-9} \text{ in}^3$$

or,

$$V_{\text{bubble}} = 4.17 \times 10^{-12} \text{ in}^3$$

The internal pressure of such a bubble, necessary for determining the density of the contained argon, would be;

$$P_{\text{internal}} = P_{\text{static}} + \frac{2\sigma}{r}$$

or,

$$P_{\text{internal}} = 4.1 + 50 = 54.1 \text{ psi}$$

thus

$$\rho_{\text{argon}} = 1.74 \times 10^{-3} \times 54/14.7 \times (2.54)^3 = \\ 0.103 \text{ gm/in}^3$$

then, each bubble would contain;

$$\text{Gas mass per bubble} = 0.103 \text{ gms/in}^3 \times 4.17 \times 10^{-12} \text{ in}^3$$

or,

$$\text{Gas mass per bubble} = 4.40 \times 10^{-13} \text{ grams of argon}$$

Thus the number of bubbles of such size would be;

$$\text{Number of 0.1 mil radius bubbles} = \frac{1.24 \times 10^{-6} \text{ gms}}{4.40 \times 10^{-13} \text{ gms/bubble}}$$

$$N = 2,820,000 \text{ bubbles}$$

Since this number of bubbles exists in 0.0125 in^3 of mercury, there are

$$2.25 \times 10^8 \text{ bubbles/in}^3.$$

Since this number is surprisingly large, and assuming that there is a possibility that the assumed bubble radius of 0.1 mils was not realistic, the same calculation was performed for bubbles with an average radius of 1 mil. Conceivably, this size of bubble is just below the visible range so that it would provide an estimate of the lower limit on the possible number of such bubbles to account for the discrepancy between gas measured and that in visible bubbles. This calculation shows that there would be 1.2×10^6 bubbles/ in^3 .

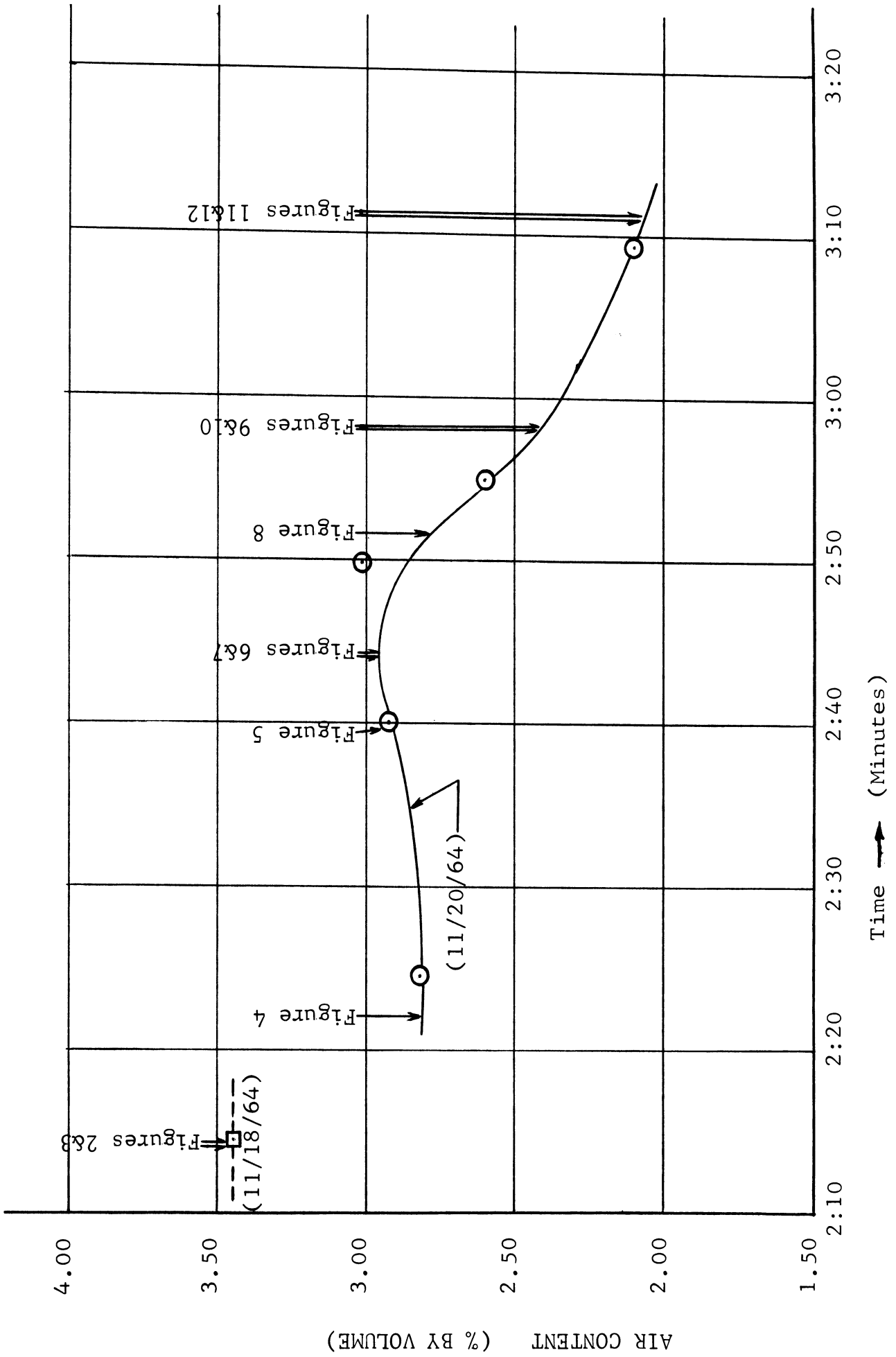


Figure 1. Air Content and Photograph Number versus Time

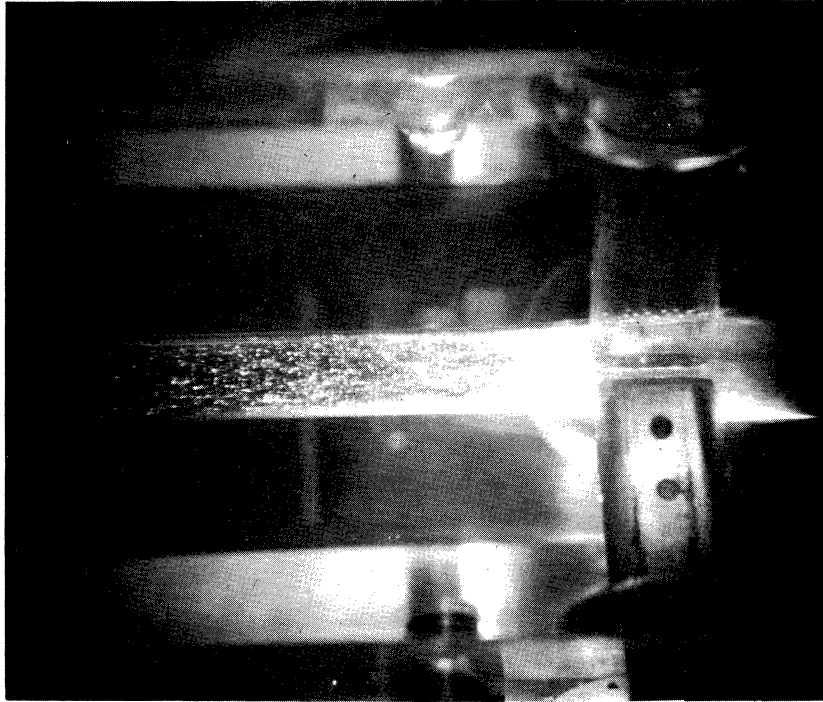


Figure 2. Photograph Number 1 of Gas Entrainment in Water Loop at 3.42% by Volume, Magnification 1X.

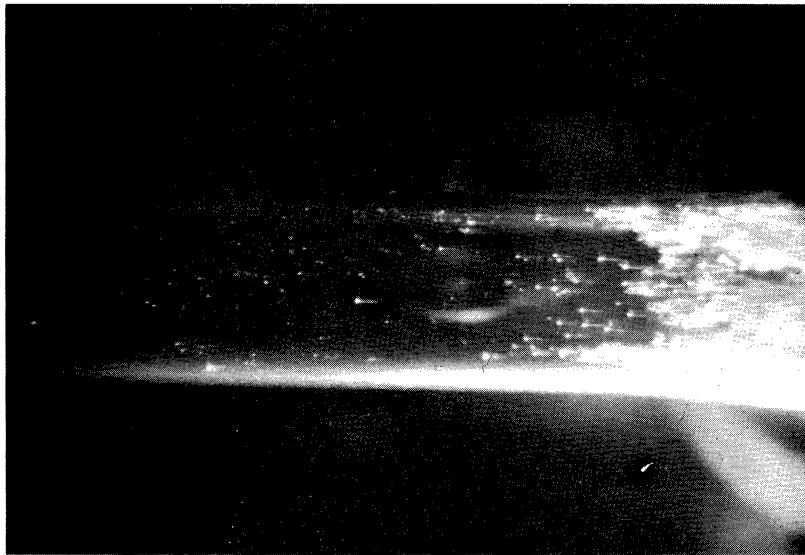


Figure 3. Photograph Number 2 of Gas Entrainment in Water Loop at 3.42% by Volume, Magnification 2X.

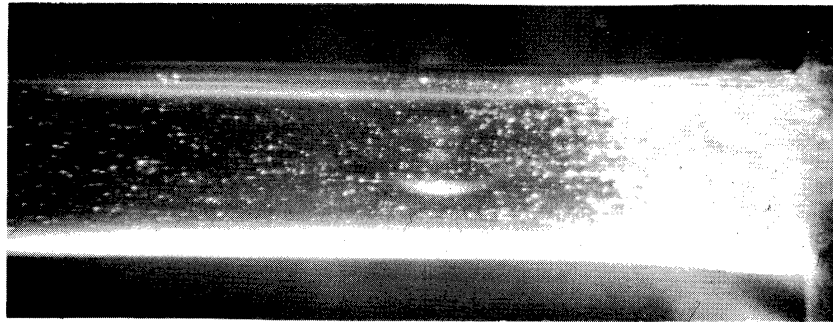


Figure 4. Photograph Number 3 of Water Loop at 2.85% by Volume Air, Magnification 2X, (11/20/64).

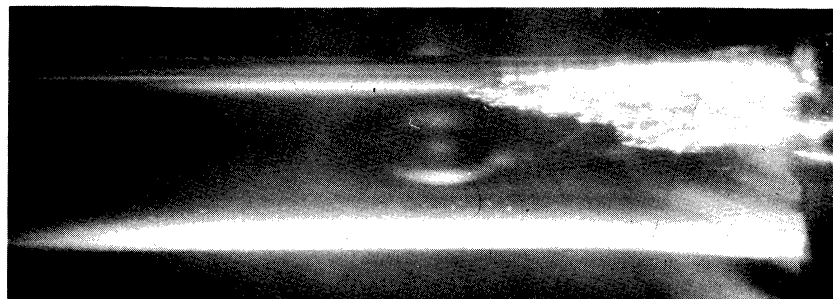


Figure 5. Photograph Number 4 of Water Loop at 2.92% by Volume Air, Magnification 2X, (11/20/64).

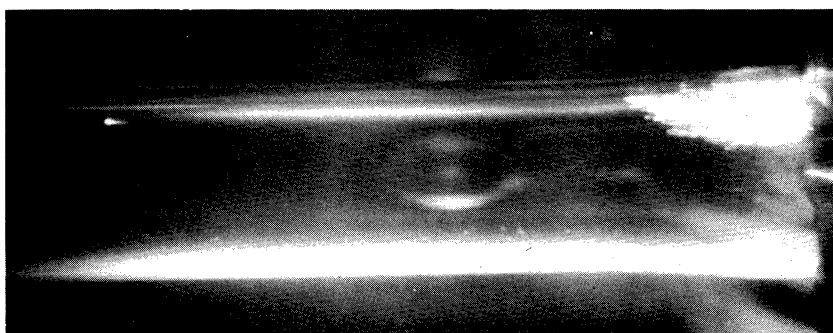


Figure 6. Photograph Number 5 of Water Loop at 2.95% by Volume Air, Magnification 2X, (11/20/64).



Figure 7. Photograph Number 6 of Water Loop at 2.95% by Volume Air, Magnification 2X, (11/20/64).

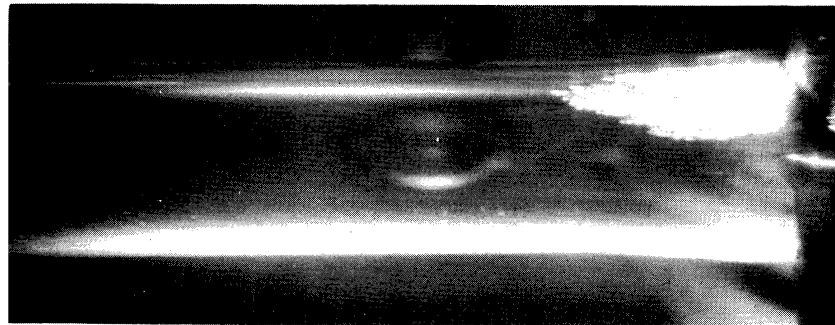


Figure 8. Photograph Number 7 of Water Loop at 2.85% by Volume Air, Magnification 2X, (11/20/64).

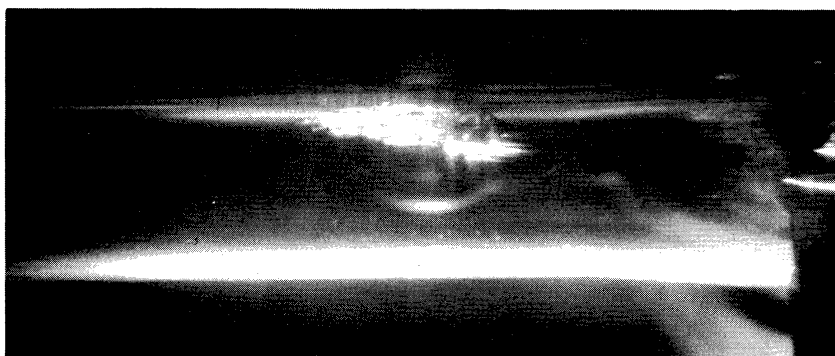


Figure 9. Photograph Number 8 of Water Loop at 2.45% by Volume Air, Magnification 2X, (11/20/64).

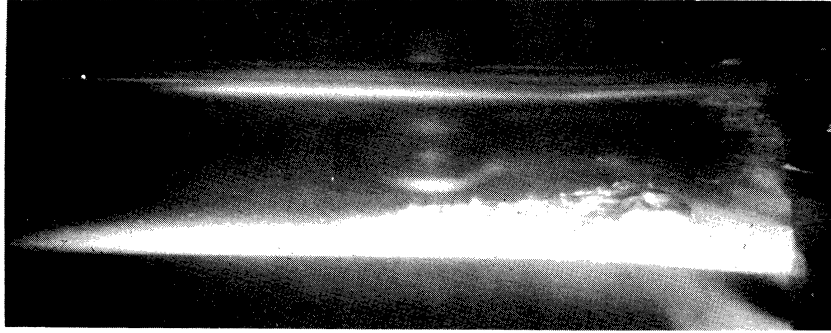


Figure 10. Photograph Number 9 of Water Loop at 2.45% by Volume Air, Magnification 2X, (11/20/64).

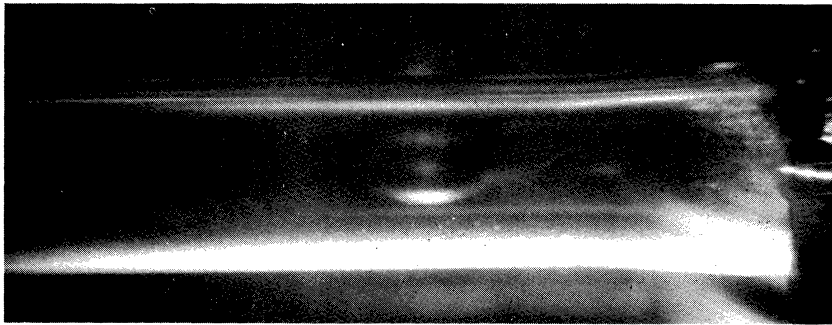


Figure 11. Photograph Number 10 of Water Loop at 2.07% by Volume Air, Magnification 2X, (11/20/64).

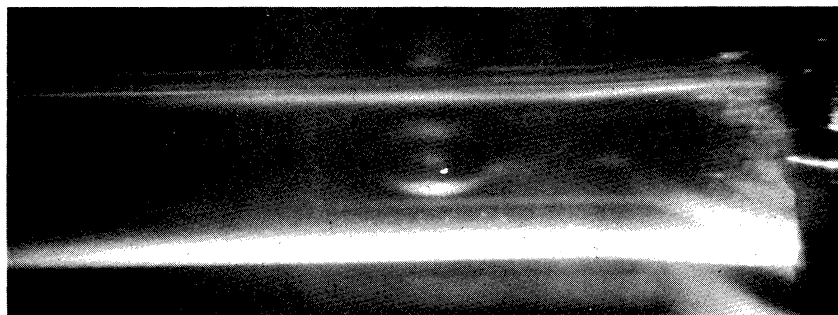


Figure 12. Photograph Number 11 of Water Loop at 2.07% by Volume Air, Magnification 2X, (11/20/64).

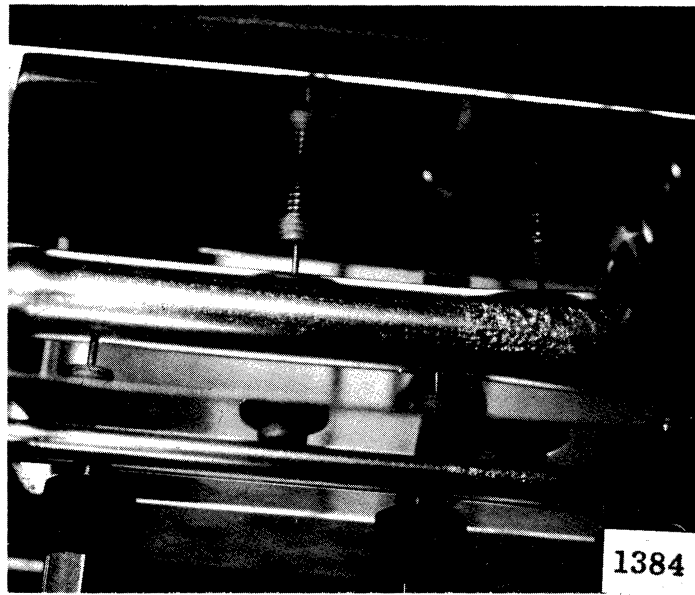


Figure 13. Standard Cavitation in Mercury at 33 ft/sec at a Gas(Argon) Content of 1.8 ppm. Average Bubble Radius in Throat is 7.9 mils. Magnification $\sim 1X$.

REFERENCES

1. Hammitt, F. G., et al., "Feasibility Investigation of Cavitation Number Measurements in Mercury and Water with Gas Injection", ORA Technical Report No. 06110-2-T, Laboratory for Fluid Flow and Heat Transfer Phenomena, Department of Nuclear Engineering, University of Michigan, July, 1964.
2. Ericson, D. M., Jr., Thesis Data, Department of Nuclear Engineering, University of Michigan, about May 22, 1964.